

# Arrays of Josephson junctions in an environment with vanishing impedance

M. Aunola, J.J. Toppari and J.P. Pekola

*Dept. of Physics, University of Jyväskylä, P.O. Box 35 (Y5), FIN-40351 Jyväskylä, Finland*

(May 19, 2019)

The Hamiltonian operator for an array of Josephson junctions with bias and gate voltages is constructed when only Cooper pair tunnelling and charging effects are taken into account. The supercurrent through the system and the pumped current induced by changing the gate voltages periodically are discussed with an emphasis on the inaccuracies in the pumping. Analytical results for the supercurrent in case of uniform arrays are obtained and compared to numerical calculations. Inhomogeneous arrays are also briefly reviewed. Some additional inaccuracies for the pumping are also considered. We use a renormalisation method for solving the relevant eigenstates for a system dominated by few low-lying basis states. The method is based on the renormalisation process used in atomic, nuclear and particle physics.

PACS numbers: 85.25.Cp, 73.40.Rw, 73.40.Gk, 73.23.Hk

## I. INTRODUCTION

When a potential well propagates adiabatically along an electron system that is effectively one-dimensional, it carries with it additional electron density, and induces dc electric current through the system. Such a pumping effect has been studied in small metallic tunnel junctions in the Coulomb blockade regime.<sup>1,2</sup> If the propagation of the potential well is arranged by phase-shifted gate voltages as in Refs. 1 and 2 and the potential well carries a quantised number  $m$  of electrons then the induced current  $I$  is related to the gating frequency  $f$  by the fundamental relation  $I = -mef$ , where  $e$  is the electron charge magnitude. These Coulomb blockade pumps transporting normal electrons have reached accuracy suitable for metrological applications.<sup>2,3</sup>

Until lately, mainly pumping of normal electrons was studied, but in a recent article<sup>4</sup> a quantitative theory of pumping Cooper pairs in gated one-dimensional arrays of Josephson junctions was presented. It was shown that quantum effects render the Cooper pair pump inaccurate in case of arrays with small junctions thus explaining the failure to demonstrate accurate pumping in the first (and so far the only) reported experiment of pumping of Cooper pairs.<sup>5</sup>

In this article we generalise the methods and results derived in Ref. 4. Higher order corrections and inhomogeneity of the array are considered in detail. We do not, however, discuss the dissipative effects induced by non-zero bias voltage.

The present method is based on the renormalisation methods used in atomic and nuclear physics.<sup>6–10</sup> In nuclear physics the method is used for creation of an effective two-body interaction which can be used for example in Shell-Model calculations. These methods can be applied to the present problem with minor modifications. Our method relies on the concept of "few-state dominance" which means, roughly speaking, that the relevant eigenstates are dominated by just a few basis states if all the rest of the states are separated from these by an energy much larger than the interaction between any of the basis states. The effects due to the other states are treated as a renormalisation of eigenstates and eigenenergies.

The article is organised as follows. In Sec. II we define "few state dominance" explicitly and explain briefly the renormalisation method we have used. In Sec. III we derive the Hamiltonian of the system and consider the pumping generally. In Sec. IV homogeneous arrays are examined in detail and analytical results are presented and compared to numerical ones. In Sec. V we examine the effects stemming from the inhomogeneity of the array. In Sec. VI we discuss how inaccuracies in the gating process affect theoretical inaccuracy and, finally we draw conclusions in Sec. VII.

## II. FEW-STATE DOMINANT SYSTEMS

### A. Structure of the Hamiltonian

The Hamiltonian describing a  $k$ -state dominant system can be written as follows.

$$H = H_0 + V, \quad H_0|l\rangle = \epsilon_l|l\rangle, \quad l = 1, 2, \dots \quad (1)$$

where we demand that

$$|\epsilon_l - \epsilon_m| \geq \Delta E, \quad \text{if } l \leq k < m, \\ |V_{nn'}| \ll \Delta E, \quad \text{for all } n, n'. \quad (2)$$

The coupling between the states is given by the residual interaction  $V$  which can often be considerably suppressed by a proper choice of the basis states. Obviously it is possible to explicitly define the quantity  $\Delta E$  as the infimum of the energy differences  $|\epsilon_l - \epsilon_m|$  but this is not necessary.

In short, there are  $k$  basis states separated from all the others by an energy  $\Delta E$  which is large as compared to the coupling between *any* two states in the system. These requirements are graphically depicted in Fig. 1 showing some of the energy levels in a  $k$ -state dominant system.

Please note that  $V_{\max}$ , the magnitude of the largest element in  $V$ , can be much smaller than the energy difference between low-lying basis states.

The low-lying eigenstates will be expanded in this  $k$ -state basis while the effects due to high-lying states are taken into account as a renormalisation of the eigenstates and eigenenergies.

## B. Renormalisation process

We will now generate an effective interaction  $\tilde{V}$  for the small space  $\{|l\rangle\}_{l=1}^k$  based on the interaction  $V$  in the full system. The renormalisation process in the context of nuclear physics is carefully explained in Refs. 6 and 7. The process is illuminative in the case of few-state dominant systems, also, and thus it will be briefly reviewed here.

Let us choose two orthogonal projection operators  $\hat{P}$  and  $\hat{Q}$  that project onto the small, active space ( $P$ -space) and the rest of the full space ( $Q$ -space), respectively, by

$$\hat{P} = \sum_{l=1}^k |l\rangle\langle l|, \quad \hat{Q} = \sum_{l(>k)} |l\rangle\langle l|. \quad (3)$$

We shall assume that  $E$  is one of the  $k$  lowest eigenenergies of the full system. Because it cannot be known in advance we shall discuss below how to estimate  $E$ .

The simplest approximation for  $\tilde{V}$  is simply  $\tilde{V} \approx \hat{P}V\hat{P}$ . The higher order corrections are obtained by letting the interaction  $V$  act between the states in the  $Q$ -space which yields

$$\tilde{V} = \hat{P} \left[ \sum_{n=0}^{\infty} \left( V \frac{\hat{Q}}{E - \hat{Q}H_0\hat{Q}} \right)^n \right] V\hat{P}. \quad (4)$$

For a  $k$ -state dominant system the series converges rather quickly since always  $\epsilon_{l(>k)} - E \gg V_{nn'}$ . Thus the expansion may be truncated at a given order, say the  $m^{\text{th}}$  order, yielding an operator  $\tilde{V}^{(m)}$ . The eigenenergies may now be solved for the effective Hamiltonian operator  $\tilde{H}^{(m)} = \hat{P}H_0\hat{P} + \tilde{V}^{(m)}$ .

The final point in the renormalisation is the choice of the eigenenergy  $E$  to be used.  $E$  should be known in advance but this is obviously impossible. The simplest choice is just the average energy

$$\bar{E} = (1/k) \sum_{j=1}^k (\epsilon_j + V_{jj}) \quad (5)$$

of the truncated Hamiltonian  $H_{\text{tr}} \equiv \hat{P}H\hat{P}$ . The results may be improved by repeatedly inserting the renormalised matrix elements  $\tilde{V}_{jj}$  into the definition of  $\bar{E}$  until self-consistency (sc) is achieved. We will call these choices as the "regular" and "regular sc" choice. Regular choices work best if the residual interaction is very weak.

The "improved" choice stands for choosing  $E$  as one of the eigenenergies  $E_j$  of  $H_{\text{tr}}$  and then diagonalising the effective Hamiltonian for the  $j^{\text{th}}$  eigenstate and eigenenergy  $\tilde{E}_j$ . If two or more states are degenerate or almost degenerate a single diagonalisation is sufficient for those states. Self-consistent "improved sc" is again obtained by repeatedly inserting  $\tilde{E}_j$  when renormalising the Hamiltonian.

A clear advantage of the "improved" choice is better accuracy in eigenenergies. The loss of orthogonality of the eigenstates in  $P$ -space is an advantage in the sense of being more realistic, and a drawback due to an increasing complexity of the problem. The  $k$ -fold renormalisation process can be handled easily. Most of the time we use the best available approach but in some cases neglecting the self-consistency allows us to give more transparent series expansions.

We suggest some additional improvements concerning the method. A few of the high-lying states may be included in the reduced  $P$ -space provided that we only wish to obtain  $k$  lowest eigenstates using the "improved" or the "improved sc" method described above. The additional levels should be those that are directly coupled to the low-lying states and provide important connections between them. Thus these connections can be included when solving the eigenvalue problem.

## C. Inverse renormalisation

The most realistic description of the problem can be obtained as follows. First one should use the renormalisation process in obtaining as precise eigenenergies  $\tilde{E}_j$  and renormalised eigenstates  $|\tilde{E}_j\rangle$  as possible. The eigenstates may then be expanded to the full space by the inverse renormalisation

$$N_j |\psi_j\rangle = |\tilde{E}_j\rangle + \left[ \sum_{n=1}^{\infty} \left( \frac{\hat{Q}V}{\tilde{E}_j - \hat{Q}H_0\hat{Q}} \right)^n \right] |\tilde{E}_j\rangle, \quad (6)$$

where  $N_j$  is a normalisation factor and  $|\psi_j\rangle$  is the eigenstate in the full space. The expanded states can be used with unrenormalised operators which is often very convenient.

The inverse renormalisation allows us to calculate matrix elements between few-state dominant eigenstates and their linear combinations reliably. For large spaces double renormalisation is often faster than even partial diagonalisation.

## III. THE COOPER PAIR PUMP

### A. General properties

An array of Josephson junctions with gate voltages, a Cooper pair pump (CPP), in the Coulomb blockade

regime is an excellent example of a few-state dominant system. In an earlier paper<sup>4</sup> the transferred charge in a homogeneous Cooper pair pump was discussed. In that article the result for the inaccuracy was derived by calculating the variance of expectation value of the number of Cooper pairs on an island far away from the island where most of the charge transfer occurs. An earlier version of the renormalisation process was also available then and it was used in order to confirm the results obtained. Additionally an analytical result for the case  $N = 3$  along a circular and triangular paths on the gate voltage plane were presented.

Figure 2 shows a schematic drawing of a gated Josephson array of  $N$  junctions ( $N$ -pump). Each junction has a capacitance  $C_k$  and a Josephson energy  $E_{J,k}$ . The phase difference over the array is  $\phi \in [0, 2\pi N]$  and the bias voltage is  $V$ . Each gate voltage  $V_{g,k}$  binds charge  $C_{g,k}V_{g,k}$  on island  $k$ . In order to (hopefully) transport exactly one Cooper pair through the array the gate voltages are operated as depicted in Fig. 2.

There are two important energy scales in a CPP. The first one is the typical Josephson coupling energy  $E_J$  related to the Cooper pair tunnelling through the junctions and the second one is the charging energy  $E_C$  related to the charging effects of the small islands between the junctions. Both are explicitly defined below. The most important parameter of the model is the ratio  $E_J/E_C$  which will be denoted by  $\varepsilon_J$ .

## B. The Hamiltonian and supercurrent operators

The Hamiltonian operator for the system can be derived explicitly after some simplifications are taken into account. Neglecting quasiparticle and other degrees of freedom the total Hamiltonian can be written as

$$H = H_C + H_J \quad (7)$$

where  $H_C$  is the charging Hamiltonian and  $H_J$  describes the Josephson tunnelling of the Cooper pairs. For an  $N$ -junction Cooper pair pump it reads

$$H_J = - \sum_{k=1}^N E_{J,k} \cos \hat{\phi}_k \quad (8)$$

where  $\hat{\phi}_k$  is the phase difference over junction  $k$ . The corresponding supercurrent operator for junction  $k$  reads

$$I_{S,k} = \frac{(-2e)E_{J,k}}{\hbar} \sin \hat{\phi}_k = \frac{-2e}{\hbar} \frac{\partial H_J}{\partial \hat{\phi}_k}. \quad (9)$$

The charging Hamiltonian  $H_C$  is diagonal in the basis formed by the charge eigenstates  $|\vec{n}\rangle$  where  $\vec{n} \equiv \{n_1, n_2, \dots, n_{N-1}\}$  and  $n_i$  is the number of Cooper pairs on each island of the array. The normalised gate voltages  $\vec{q} \equiv \{q_1, q_2, \dots, q_{N-1}\}$  where  $q_k = -V_{g,k}C_{g,k}/2e$  may be considered as parameters in  $H_C$ . The charging energy for

a given state depends only on the quantity  $\vec{u} = \vec{n} - \vec{q}$  and is evaluated below.

Although we can not take into account the dissipative effects induced by non-zero bias voltage  $V$ , the calculation of the charging energy is more transparent if  $V$  is included. First we evaluate only the capacitive charging energy of  $N$  tunnel junctions and include the work done by the voltage source in the end. Let  $v_k$  denote the charge over the junction  $k$  in units  $-2e$ . The free charge on island  $k$  to be distributed between junctions  $k$  and  $k+1$  is  $u_k = n_k - q_k$  in the same units. The capacitive charging energy of these  $N$  junctions is simply

$$E_{ch, cap} = \sum_{k=1}^N \frac{(2e)^2 v_k^2}{2C_k}. \quad (10)$$

We define the typical charging energy  $E_C = (2e)^2/2C$  and ratios  $c_k = C_k/C$  where the "average" capacitance  $C$  is given by  $C = N \left( \sum_{k=1}^N (1/C_k) \right)^{-1}$ . For a homogeneous array  $c_k \equiv 1$ . The conservation of charge now requires

$$v_k - v_{k+1} = u_k \quad (11)$$

which is satisfied by  $v_k = \tilde{v}_k + y$  with still undetermined  $y$  and

$$\tilde{v}_k = \sum_{j=k}^{N-1} u_j - \frac{1}{N} \sum_{j=1}^{N-1} j u_j \quad (12)$$

for which  $\sum_{k=1}^N \tilde{v}_k = 0$  holds. Thus  $\tilde{v}_k$  represent the pure redistribution of charge on islands and  $y$  represents the common amount of charge that the bias voltage pushes through all junctions. Using  $(-2e)/C$  as the unit of voltage allows us to rewrite the condition that bias voltage is the sum of voltages over junctions as  $\tilde{V} = \sum_{k=1}^N (v_k/c_k)$  from whence we obtain the simple result  $y = [\tilde{V} - \sum_{k=1}^N (\tilde{v}_k/c_k)]/N$  (note that  $y$  may be non-zero even if  $\tilde{V} = 0$  for an inhomogeneous array). Inserting  $y$  into the expression for the capacitive energy yields

$$E_{ch, cap} = E_C \left[ \sum_{k=1}^N \frac{\tilde{v}_k^2}{c_k} - \frac{1}{N} \left( \sum_{k=1}^N \frac{\tilde{v}_k}{c_k} \right)^2 \right] + \frac{CV^2}{2N} \quad (13)$$

with  $\tilde{v}_k$  defined in Eq. (12). The work done by the voltage source has to be included in the energy and it reads

$$- \frac{CV^2}{N} + E_C \frac{2\tilde{V}}{N} \sum_{k=1}^N \frac{\tilde{v}_k}{c_k}. \quad (14)$$

We finally obtain the total charging energy

$$E_{ch} = E_C \left[ \sum_{k=1}^N \frac{\tilde{v}_k^2}{c_k} - \frac{L^2 - 2L\tilde{V}}{N} \right] - \frac{CV^2}{2N} \quad (15)$$

where  $L \equiv \sum_{k=1}^N (\tilde{v}_k/c_k)$ . The term  $-\frac{1}{2}(C/N)V^2$  is independent of the charge eigenstate so its contribution to the energy differences is zero. Thus we find that for a homogeneous array the charging energy differences are independent of biasing.

For zero bias voltage the term in parenthesis is invariant under the transformation  $\{\tilde{v}_k\} \rightarrow \{v_k\}$  where  $v_k = \tilde{v}_k + x$  for arbitrary  $x$ . This means that the energy differences may be evaluated for any (convenient) solution of Eqs. (11). This is very advantageous since it is most convenient to index the intermediate states by the number of required jumps when using our renormalisation procedure.

It is obviously more convenient to work in the basis of charge eigenstates which is fortunately possible. Instead of the phases,  $\phi_k$ , and the number of tunnelled pairs through each junction  $m_k$  we may use the the number of Cooper pairs on each island  $n_k$  and the respective phases  $\theta_k$ . This set must be augmented by the total phase difference over the array  $\phi = \sum_{k=1}^N \phi_k$  and the average number of tunnelled Cooper pairs in the array  $\mathcal{N} = (1/N) \sum_{k=1}^N m_k$ . Naturally  $\phi$  is periodic over  $2N\pi$  and the eigenvalues of  $\mathcal{N}$  are multiples of  $1/N$ .

Since the model Hamiltonian is independent of  $\mathcal{N}$ ,  $\phi$  is a constant of motion and we will augment the charge eigenstate basis with  $\phi$  to obtain the set  $\{|n_1 n_2 \dots n_{N-1} \phi\rangle\}$ . The value of  $\phi$  is related to the external bias voltage by the relation  $d\phi/dt = -(2e)V/\hbar$ . The oscillation frequency of  $\phi$  is approximately  $V [\mu\text{V}] \cdot 0.5 \text{ GHz}$ . This article concerns the case when  $\phi$  is locked ( $V = 0$ ) since we can not yet take into account the dissipative effects that biasing induces.

In the above-mentioned basis the Hamiltonian has the form

$$H = H_C(\vec{q}) - \sum_{\vec{n}, k=1}^N \frac{E_{J,k}}{2} (|\vec{n} + \delta_k\rangle \langle \vec{n}| e^{i\phi/N} + \text{H.c.}) \quad (16)$$

where the tunnelling vector  $\vec{\delta}_k$  describes the change of  $n$  due to tunnelling of one Cooper pair through the  $k^{\text{th}}$  junction. The non-zero components of  $\vec{\delta}_k$  are (if applicable)  $(\vec{\delta}_k)_k = 1$  and  $(\vec{\delta}_k)_{k-1} = -1$ . Each tunnelling in the 'forward' direction is thus associated with a phase  $e^{i\phi/N}$ . The phases  $\phi_k$  related to single tunnel junctions are subject to a large uncertainty if the Hamiltonian is dominated by the charging Hamiltonian  $H_C(\vec{q})$ .

The supercurrent operator related to the tunnelling through the  $k^{\text{th}}$  junction can be written as

$$I_{S,k} = \frac{(-2e)E_{J,k}}{2\hbar} \sum_{\vec{n}} (-i|\vec{n} + \delta_k\rangle \langle \vec{n}| e^{i\phi/N} + \text{H.c.}) \quad (17)$$

The quantity  $(-2e)E_{J,k}/\hbar$  is the critical current  $I_{c,k}$  of junction  $k$ . We also define the (average) supercurrent operator  $I_S$  by

$$I_S = \frac{1}{N} \sum_{j=1}^N I_{S,k} = \frac{(-2e)}{\hbar} \frac{\partial H}{\partial \phi}, \quad (18)$$

where the last equality follows from the  $\phi$ -independence of  $H_C$  and the relation between  $\phi_k$  and  $\phi$ . The common expectation value of  $I_S$  and  $I_{S,k}$  in a stationary state  $|E_m\rangle$  is given by  $(-2e/\hbar)\partial E_m/\partial \phi$ . Since  $I_S$  can be expressed as a derivative of the full Hamiltonian operator its matrix element between two different stationary states  $|m\rangle$  and  $|n\rangle$  for a given phase difference  $\phi_0$  can be expressed simply as

$$\langle m|I_S|n\rangle = \frac{(-2e)(E_m - E_n)}{\hbar} \lim_{d\phi \rightarrow 0} \frac{\phi_0 \langle m|n\rangle_{\phi_0+d\phi}}{d\phi}, \quad (19)$$

where  $E_m$  and  $E_n$  are the eigenenergies related to these states. In the derivation of the above equation one has to use the definition of the derivative as a limiting value.

### C. The supercurrent and the transferred current

As shown in the previous article<sup>4</sup> there are two mechanisms of Cooper pair transfer in the array. The first one is direct supercurrent through the whole array due to non-zero  $\phi$  and the other one is pumping, the charge transfer in response to the adiabatic variation of the injected charges  $\vec{q}$ .

The expressions for these mechanisms can be derived as follows. For each  $t$  we introduce the basis of instantaneous eigenstates  $\{|m_{(t)}\rangle\}$  with eigenenergies  $\{E_m\}$  of the full Hamiltonian (7) for a given  $\vec{q}(t)$ . Assuming slowly varying gate voltages we may solve time-dependent Schrödinger equation with the initial condition  $|\psi(t_0)\rangle = |m_{(t_0)}\rangle$  to obtain

$$\begin{aligned} |\psi_{(t_0+\delta t)}\rangle &= e^{-iE_m\delta t/\hbar} |m_{(t_0)}\rangle \\ &+ \sum_{l(\neq m)} \frac{(e^{-iE_l\delta t/\hbar} - e^{-iE_m\delta t/\hbar}) \langle E_l | \vec{\nabla}_{\vec{q}} \cdot \frac{\partial \vec{q}}{\partial t} | l_{(t_0)} \rangle}{i(E_l - E_m)/\hbar} |l_{(t_0)}\rangle \\ &\equiv |m_{(t_0)}\rangle + |\delta m_{(\delta t)}\rangle. \end{aligned} \quad (20)$$

Here the term  $|\vec{\nabla}_{\vec{q}} \cdot \frac{\partial \vec{q}}{\partial t}\rangle$  is the directional derivative of the ground state with respect to the change in  $\vec{q}$ . The amount of charge  $Q$  that passes through junction  $k$  during a short time interval  $\delta t$  is then

$$\begin{aligned} \delta Q &= \int_{t_0}^{t_0+\delta t} \langle \psi_{(t)} | I_{S,k} | \psi_{(t)} \rangle dt = \delta t \langle I_{S,k} \rangle_{|m_{(t_0)}\rangle} \\ &+ 2\text{Re} \left[ \int_{t_0}^{t_0+\delta t} \langle m_{(t_0)} | I_{S,k} | \delta m_{(t-t_0)} \rangle dt \right], \end{aligned} \quad (21)$$

where we have neglected the term quadratic in  $|\delta m\rangle$  and oscillatory terms by assuming that  $\delta t \gg \hbar/(E_l - E_m)$  holds for all  $l$ . The first part describes charge transfer by the direct supercurrent. The induced charge transfer can be integrated out yielding

$$\delta Q_{k,\text{ind}} = -2\hbar \sum_{l(\neq m)} \text{Im} \left[ \frac{\langle m | I_{S,k} | l \rangle \langle l | \delta m \rangle}{E_l - E_m} \right] \quad (22)$$

where  $|\delta m\rangle$  is the change in the instantaneous eigenstate induced by the change  $\vec{q}(t_0) \rightarrow \vec{q}(t_0 + \delta t)$ . If the new instantaneous eigenstate is obtained by diagonalisation methods its phase must match the original one.

For a closed path  $\gamma$  the total transferred charge must be equal for all  $N$  junctions so the total transferred charge can be written in terms of the average supercurrent operator  $I_S$ . The total transferred charge  $Q$  over a pumping period  $\tau$  is given by

$$\frac{Q}{-2e} = \frac{1}{\hbar} \int_0^\tau \frac{\partial E_m(t)}{\partial \phi} dt - \frac{2\hbar}{-2e} \oint_{\gamma} \sum_{l(\neq m)} \text{Im} \left[ \frac{\langle m|I_S|l\rangle \langle l|dm\rangle}{E_l - E_m} \right] \quad (23)$$

where  $|dm\rangle$  is the differential change of  $|m\rangle$  due to a differential change of the gate voltages  $d\vec{q}$ . By using Eq. (19) the pumped charge for the state  $|m\rangle$  may be expressed simply as

$$\frac{Q_p}{-2e} = 2 \oint_{\gamma} \sum_{l(\neq m)} \text{Im} \left[ \lim_{\phi' \rightarrow \phi_0} \frac{\phi_0 \langle m|l\rangle_{\phi'}}{\phi' - \phi_0} \langle l|dm\rangle \right]. \quad (24)$$

Thus the pumped current is mediated by the induced mixing of other components into the initial state ( $\langle l|dm\rangle$ ) and modified by the rate of change of relative phase between these states. The pumped charge is independent of the total phases of energy eigenstates as required. This formulation is especially effective in the regime of two-state dominance.

The pumped charge resulting from the induced corrections depends only on the chosen path while the amount of charge that passes through the system due to supercurrent also depends on the speed of the gating because it is proportional to an integral over time.

The transferred charge may also be considered from another point of view. As pointed out in Ref 4, the average number of Cooper pairs on each island  $\langle n_k \rangle$  is strictly linked to the amount of charge that has passed through junctions  $Q_k$  during a short time interval by the relation  $\delta \langle n_k \rangle = Q_k - Q_{k+1}$ . In the Coulomb blockade regime the average numbers may be evaluated reliably which will be done later.

We will postpone the detailed analysis till Sec. VI but now we only point out that due to the symmetry of the charging energy the estimate for the transferred charge is exactly  $-2e$  for the saw-tooth gating regardless of the uniformity of the array. We will also show that for longer arrays the pumping inaccuracy can be strongly suppressed but one will need high-accuracy gating to be certain that other sources of inaccuracy will not mask their contribution.

From here on we shall almost exclusively be interested in uniform arrays of  $N$  tunnel junctions although the renormalisation can be performed for a non-uniform Cooper pair pump by using the general expression of the charging energy (15). The results can not be written as compactly as for the homogeneous case but the results will still retain the general features.

## IV. THE HOMOGENEOUS COOPER PAIR PUMP

### A. Properties of the charging Hamiltonian $H_C(\vec{q})$

For uniform arrays of  $N$  junctions all Josephson energies are equal to  $E_J$ . The magnitude of the largest coupling matrix element is simply  $E_J/2$  so the condition for few-state dominance is that the energy gap between the low-lying and high-lying states must be larger or much larger than  $E_J$ .

We shall now examine the properties and the symmetries of the charging Hamiltonian  $H_C(\vec{q})$  in the absence of external bias. For a homogeneous pump the expression for the charging energy simplifies to

$$E_{\vec{v}}^{\vec{u}} = E_C \left[ \sum_{k=1}^N v_k^2 - \frac{1}{N} \left( \sum_{k=1}^N v_k \right)^2 \right], \quad (25)$$

where the coefficients  $v_k$  are solutions of Eqs. (11). Let  $\{w_k\}_{k=1}^m$  denote the different, non-zero components of  $\vec{v}$  and  $\{s_k\}_{k=1}^m$  be their multiplicities. The charging energy can then be written as

$$E_{\vec{v}}^{\vec{u}} = E_C \left[ \sum_{k=1}^m s_k w_k^2 - \frac{1}{N} \left( \sum_{k=1}^m s_k w_k \right)^2 \right]. \quad (26)$$

Because the order of the components  $v_k$  is immaterial, we define a vector  $(s)$  as a sum of  $s$  different tunnelling vectors  $\vec{\delta}_j$ . There are  $N!/s!(N-s)!$  different vectors of this type but for purposes of the charging energy they are equivalent. Two different vectors  $(s_1)$  and  $(s_2)$  may be unambiguously summed only if they do not include any identical tunnelling vectors.

Since the number of Cooper pairs on each island may obtain only integer values the degree of symmetry of  $H_C(\vec{q})$  depends on how exactly  $\vec{q}$  matches with the set  $\{\vec{n}\}$ . From here on we use the symbol  $E_{\vec{n}} \equiv E_{\vec{v}}^{\vec{n}-\vec{q}}$  to denote the charging energy of the state  $|\vec{n}\rangle$  for a fixed value of the gate voltages.

The highest symmetry is obtained when  $\vec{q} = \vec{n}_0$  for a certain charge eigenstate  $|\vec{n}_0\rangle$ . From above we obtain  $E_{\vec{n}_0} = 0$  and

$$E_{\vec{n}_0+(s)} = E_{\vec{n}_0-(s)} = E_C s(N-s)/N. \quad (27)$$

In terms of the charge eigenstates only  $|\vec{n}_0+(s)\rangle = |\vec{n}_0-(N-s)\rangle$  but the direction of the jumps will be important when considering the tunnelling Hamiltonian  $H_J$ .

We find that if  $E_J \ll E_C$  the Cooper pair pump is single-state dominant at  $\vec{q} = \vec{n}_0$  and in its vicinity. The supercurrent may be evaluated easily since no diagonalisation is necessary. One only needs to evaluate the single matrix element in  $\hat{V}$  and derive it for the supercurrent. Self-consistency improves the agreement for larger values of  $\varepsilon_J$ .

Moving in a direction of one of the tunnelling vectors preserves also a great deal of symmetry. For brevity we

use  $r$  to stand for  $\vec{\delta}_r$ . The vectors  $(s)$  may not include  $\vec{\delta}_r$  so the state  $|\vec{n}_0 + 2r + (s)\rangle$  is reached from  $|\vec{n}_0\rangle$  by tunnelling twice through junction  $r$  and once through  $s$  other junctions. At the half-way point  $\vec{q} = \vec{n}_0 + \frac{1}{2}\vec{\delta}_r$  states  $|\vec{n}_0 + \vec{n}'\rangle$  and  $|\vec{n}_0 + r - \vec{n}'\rangle$  are degenerate for all  $\vec{n}'$ . Near the degeneracy point the system is two-state dominant. This limit is the most relevant one for us since it is realised by saw-tooth gating as shown in Fig. 2.

The Hamiltonian is also highly symmetric at the resonance point  $\vec{q} = (1/N, 1/N, \dots, 1/N)$ , where the states  $\{|\sum_{j=1}^k \vec{\delta}_j\rangle\}_{k=1}^N$  become degenerate. The system becomes  $N$ -state dominant with the well-known nearest-neighbour coupling and the supercurrent was shown to behave as  $\sin(\phi/N)/N$ . Because  $\varepsilon_J$  is not zero, the supercurrent will be renormalised by the coupling to the other states. This renormalisation will be evaluated in the next subsection.

## B. Pumped charge and supercurrent

We will now evaluate the inaccuracy in the pumping for the uniform array when gate voltages are operated as depicted in Fig. 2. Due to the symmetry of the charging Hamiltonian  $H_C$  it is enough to consider any one of the legs and multiply the results by  $N$ . In the Coulomb blockade regime the system is always dominated by either one or two charge eigenstates only. The pumping mainly occurs when these two states are nearly degenerate.

Let us consider a two-level system with a Hamiltonian

$$H = \begin{pmatrix} \epsilon_1 & -ve^{-i\theta(\phi)} \\ -ve^{i\theta(\phi)} & \epsilon_2 \end{pmatrix}. \quad (28)$$

For the truncated system with only two charge eigenstates  $\theta(\phi) = \phi/N$  and  $v = E_J/2$ . Diagonal elements are the charging energies  $E_{\text{ch}}^{(1)}$  and  $E_{\text{ch}}^{(2)}$  for these states. The renormalised Hamiltonian  $\tilde{H}$  can be decomposed as

$$\tilde{H} \approx \begin{pmatrix} E_{\text{ch}}^{(1)} - a^{(1)} \cdot E_C & v|b(\phi)|e^{-i(\phi/N+\phi_b)} \\ v|b(\phi)|e^{i(\phi/N+\phi_b)} & E_{\text{ch}}^{(2)} - a^{(2)} \cdot E_C \end{pmatrix} \quad (29)$$

where  $v = -E_J/2$ ,  $a^{(j)} = a_0^{(j)} + a_1^{(j)} \cos \phi$ ,  $j = 1, 2$ ,  $b = b_0 + b_{-1}e^{-i\phi} + b_1e^{i\phi}$  and  $e^{i\phi_b} = b/|b|$ . The leading components for these coefficients are  $a_0 \propto \varepsilon_J^2$ ,  $a_1 \propto \varepsilon_J^N$ ,  $b_0 \approx 1 + c\varepsilon_J^2$ ,  $b_{-1} \propto \varepsilon_J^{N-2}$  and  $b_1 \propto \varepsilon_J^N$ . The actual values for these parameters are discussed below. This is a reasonable decomposition as the next corrections would be  $a_2$  and  $b_{\mp 2}$  which are further suppressed by  $\varepsilon_J^N$ . The same decomposition may be used for an inhomogeneous pump but the renormalisation process is more complicated.

In order to calculate the integral (24) for the leg in pumping we will use a parameter  $\eta = (\epsilon_1 - \epsilon_2)/2v$  which is linear in gate charge  $\vec{q}$  for the truncated system and almost linear for the renormalised system. The gating induced correction for the ground state yields a term

$\langle 2|d1\rangle = \frac{1}{2}d\eta/(1 + \eta^2)$  which is real. Thus we only need the imaginary part of the limit in (24) which reads

$$\text{Im} \left[ \lim_{d\phi \rightarrow 0} \frac{\phi_0 \langle 1|2\rangle_{\phi_0+d\phi}}{d\phi} \right] = -\frac{d\theta/d\phi}{2\sqrt{1+\eta^2}}. \quad (30)$$

For the truncated system  $d\theta/d\phi = 1/N$  and the pumped charge is

$$\frac{Q_p}{-2e} = \frac{1}{2N} \left[ \frac{\eta_i}{\sqrt{1+\eta_i^2}} - \frac{\eta_f}{\sqrt{1+\eta_f^2}} \right]. \quad (31)$$

The symmetry of the Hamiltonian implies that the pumped charge for the full cycle with  $N$  legs should be exactly  $-2e$ . In the limit  $\varepsilon_J \rightarrow 0$  this result obviously holds. First we have neglected the charge transfer induced by higher excited states. Also one must remember that the final state of the current leg becomes the initial state of the next one. Simultaneously a new state appears as the final state. This change is certainly associated with some charge transfer so we bluntly assume that without renormalisation  $Q_p = -2e$ .<sup>1</sup>

For the renormalised system  $d\theta/d\phi$  may be evaluated analytically and the result is

$$\frac{d\theta_{\text{ren}}}{d\phi} = \frac{1}{N} + \frac{b_0(-b_{-1} + b_1) \cos \phi - b_{-1}^2 + b_1^2}{|b(\phi)|^2}. \quad (32)$$

The most important correction is  $-b_0 b_{-1} \cos \phi / |b|^2$  which is proportional to  $\varepsilon_J^{N-2}$  as shown in Ref. 4. Since  $b \approx 1$  it is still reasonable to assume that the term  $1/N$  still carries the charge  $-2e/N$  over a single leg. Thus the pumping inaccuracy may be evaluated as the weighted average of  $N d\theta/d\phi$  on a single leg. These coefficients are obtained by using the “regular sc” choice for the eigenenergy  $E$  in the renormalisation. Our renormalisation includes all terms up to the third order and coefficients  $a_1$  and  $b_{\mp 1}$  up to and including order  $\varepsilon_J^N$ .

For practical purposes it is often accurate enough to evaluate Eq. (32) at the degeneracy point. If  $\varepsilon_J$  is small then  $d\theta/d\phi$  changes considerably but the weight is concentrated around the degeneracy point. For larger values of  $\varepsilon_J$  we find that  $d\theta/d\phi$  is more stable.

In Fig. 3 the renormalised and numerical inaccuracies for  $N = 3$  are shown. The basis consists of those 41 states that satisfy  $|n_1| + |n_2| \leq 4$ . The case  $N = 3$  was chosen because the deviations from the basic result  $Q_p/(-2e) = 1 - Nb_{-1} \cos \phi$  are largest for reasonable values of  $\varepsilon_J$ . The

<sup>1</sup>In principle, it is possible to evaluate the charge transfer integral more accurately by using the renormalisation process in order to find the explicit wave functions of the  $4N$  lowest eigenstates at the degeneracy point and its vicinity. The increase in the accuracy is in no proportion to the increase in the complexity of the problem, though.

maximum value for the numerical and analytical pumped charges are 2.14 and 2.18, 2.87 and 2.98, 3.70 and 3.89 for the cases  $\varepsilon_J = 0.1, 0.15$  and  $0.2$ , respectively. The previous result<sup>4</sup> was a simple law  $Q_{\text{pump}}/(-2e) = 1 - 9\varepsilon_J \cos \phi$  so the improvement is remarkable.

The above result suggests that although the supercurrent on the gating path for phase differences  $\phi = 0$  and  $\pi$  is essentially zero they could be distinguished by pumping and measuring the current if  $\varepsilon_J > 0.02$ . The ratio between the pumped currents will in addition yield an estimate for  $\varepsilon_J$ . Even impedance of the environment does not necessarily erase this signature though it may be modified.

By defining quantities  $\epsilon_j = E_{\text{ch}}^{(j)}/E_C - a^{(j)}$ ,  $j = 1, 2$ , the eigenenergies of the renormalised system can be expressed simply as

$$\begin{aligned} \tilde{E}_1/E_C \\ \tilde{E}_2/E_C \end{aligned} \left\{ \right. = \frac{\epsilon_1 + \epsilon_2}{2} \mp \frac{1}{2} \sqrt{(\Delta\epsilon)^2 + \varepsilon_J^2 |b(\phi)|^2} \quad (33)$$

where  $\Delta\epsilon \equiv \epsilon_1 - \epsilon_2$ . The supercurrent flowing in the ground state then reads

$$\langle I_S \rangle_{\text{g.s.}} = (I_c \sin \phi) \left[ \frac{a_1^{(1)} + a_1^{(2)}}{2q} \right. \\ \left. + \frac{b_0(b_{-1} + b_1) + 2b_{-1}b_1 \cos \phi - (a_1^{(1)} - a_1^{(2)})\Delta\epsilon/\varepsilon_J}{(2/q)\sqrt{(\Delta\epsilon)^2 + \varepsilon_J^2 |b(\phi)|^2}} \right]. \quad (34)$$

In Fig. 4 the renormalised and numerical supercurrent are shown for  $N = 5$ . The supercurrent is reproduced well in all cases. The 40 state basis used is too small to produce the supercurrent fully even in the lowest order but it was chosen for and to show that the renormalisation also works for restricted bases which will be discussed in Sec. IV C. We naturally used “improved sc” choice when evaluating the supercurrent in the ground state.

The renormalisation of the supercurrent at the resonance point  $\vec{q} = (1/N, 1/N, \dots, 1/N)$  has also been calculated. The well-known basic result for  $N$  degenerate levels with nearest-neighbour coupling is  $I_{S,0} \equiv \langle I_S \rangle = I_c \sin(\phi/N)/N$ . Here  $\phi \in (-\pi, \pi]$  and the current is  $2\pi$ -periodic because at  $\phi = \pi$  the ground state energy begins to decrease again. Naturally this jump is instantaneous in theory only.

The previous result is modified because  $N$  degenerate states are coupled to other states also. The most transparent way is to express the actual supercurrent in units  $I_{S,0}$  for all  $N$ . The nearest groups of  $N$  levels lie at the charging energies  $2E_C/N$  and  $4E_C/N$  above these degenerate levels. Thus these energy differences become very small for larger  $N$  and the importance of higher order corrections becomes more pronounced even at small  $\varepsilon_J$  as seen from Fig. 5. In the limit  $\varepsilon_J \rightarrow 0$  the correction is linear and reads  $Nq \cos(\phi/N)$ . For  $N > 6$  the renormalisation factor is larger than 2 at  $\varepsilon_J = 0.2$ . This renormalisation will modify but not cancel the overall suppression  $1/N^2$  of the maximal supercurrent. In the

next subsection we will discuss the basis effects on the resonance current.

### C. Effects due to restricted bases

Because unlimited bases cannot be used due to the limitations of the computing resources, we shortly describe the different types of bases we have used and their motivations. There are three classes denoted as a-, b- and c-bases. A class a-basis includes all those states that contribute to the pumping inaccuracy in the lowest order  $\varepsilon_J^{N-2}$ . A class b-basis produces the full supercurrent in the lowest order and a class c-basis includes all terms in coefficients  $a_1$  and  $b_{\pm 1}$  up to and including order  $\varepsilon_J^N$ . In some cases some modification of these bases has been used due to computational necessities.

An a-basis is constructed as follows. If junction  $k$  connects the degenerate states in the current leg the final charge eigenstate can be reached by going through all other  $N - 1$  junctions in the backward direction in an arbitrary order. There are thus  $2^{N-2} - 1$  intermediate states for each leg. This means that there are altogether  $2^{N-2}N$  states in a class a-basis. The 40-state basis in Fig. 4 is an example of such a basis.

A b-basis must include all intermediate states that are visited when a Cooper pair tunnels once through all  $N$  junctions in an arbitrary order. A similar argument as in the previous case shows that the total number of states in a b-basis is  $2^{N-1}N$ . The inaccuracy calculations for  $N = 5$  have been done mainly using an 80-state basis. This difference is clearly shown in Fig. 4 and it will be discussed in the next section when we take a look at pumping in inhomogeneous arrays.

Finally c-basis includes all the previous paths plus those paths including an additional pair of tunnellings through one junction in forward and backward directions. No known formula for the number of states exists but a c-basis includes 100, 325, 966, 2695 and 7176 states in cases  $N = 4$  to  $N = 8$ , respectively. These are obviously too cumbersome for the calculation of inaccuracy and in case  $N = 8$  they are presently too large to diagonalise due to memory restrictions. They have been used in calculating the supercurrent in Fig. 5.

From here on we reserve the superscript in parenthesis  $(k)$  for the  $\varepsilon_J^k$ -dependent part of any coefficient and the distinction between charge eigenstates 1 and 2 is taken to be complied implicitly. The differences between these bases can be described conveniently by considering the values of the renormalisation parameter at the degeneracy point in case of the saw-tooth gating. The differences arise from the inclusion and exclusion of different states. From the point of view of the inaccuracy the  $\varepsilon_J^2$ -dependent terms in  $a_0$  and  $b_0$  act against inaccuracy, the first one by increasing the energy denominator and the second one by decreasing the phase variation in the  $d\theta/d\phi$ . Coefficient  $b_1$  is very small in the order  $\varepsilon_J^N$  while

$b_{-1}$  is relatively large. Naturally  $b_{-1}$  produces the main component of the inaccuracy in the order  $\varepsilon_J^{N-2}$  and the same component reduces the inaccuracy in combination with  $a_0$ .

The analytical expression for the lowest order component  $b_{-1}^{(N-2)}$  was already given in Ref. 4 and it reads  $(N/2)^{N-2}(N-1)/(N-2)!$ . The  $\varepsilon_J^2$ -dependent terms in coefficients  $a_0$  and  $b_0$  read

$$\begin{aligned} a_{0,a}^{(2)} &= \frac{N-2}{4} + \frac{N(N-1)}{4(N-2)}, \\ a_{0,b+}^{(2)} &= \frac{N-1}{4} + \frac{N(N-1)}{4(N-2)} + \frac{N}{4(2N-2)}, \\ b_{0,a}^{(2)} &= N/2, \\ b_{0,b+}^{(2)} &= N(N-1)/2(N-2), \end{aligned}$$

where index a corresponds to an a-basis and b+ to a b-basis or larger. In both cases an a-basis lacks one pair of neighbours that are included in calculation of the lowest order corrections.

The analytical expressions for the  $\varepsilon_J^N$ -dependent terms in  $b_{\pm 1}$  are composed of several multiple summations. For completeness we have tabulated the values of these coefficients for different bases in Table I. Since  $b_1$  is so small only the full value is given. Using all the above mentioned coefficients a power expansion of the pumped charge up to the order  $\varepsilon_J^N$  may be expressed as

$$\begin{aligned} \frac{Q_p}{-2e} &\approx 1 - N\varepsilon_J^{N-2} \cos \phi \left[ b_{-1}^{(N-2)} \right. \\ &\quad \left. + \varepsilon_J^2 \left( b_{-1}^{(N)} - b_1^{(N)} - (Nl(N)a_0^{(2)} + b_0^{(2)})b_{-1}^{(N-2)} \right) \right] \quad (35) \end{aligned}$$

where  $l(N) \approx 1$  comes from the energy denominators. Its value is 1, 1, 11/12, 5/6 and 137/180 in cases  $N = 3$  to  $N = 7$ , respectively. The inaccuracy scales dominantly as  $\varepsilon_J^{N-2} \cos \phi$  which is the scaling we have used when depicting the inaccuracy for  $N \geq 5$ .

In cases  $N = 3$  and  $N = 4$  terms  $3(b_{-1}^{(1)})^2 \varepsilon_J^2 \cos^2 \phi - 3(b_{-1}^{(1)})^3 \varepsilon_J^3 \cos^3 \phi$  and  $4(b_{-1}^{(2)})^2 \varepsilon_J^4 \cos^2 \phi$  are also required. The importance of the terms for  $N = 3$  can be seen from Fig. 3. The above mentioned expansion works reasonably well up to  $\varepsilon_J \approx 0.1$ .

We are taking a closer look at the case  $N = 5$  in Fig. 6 where the power expansions for b- and an almost full c-basis are compared to numerical results for  $\phi = 0$ . In addition the third order renormalisation result is shown. The value of coefficient  $b_{-1}^{(N)}$  for our 240-state basis is 123.1 just 2 % short of the full c-basis value 125.54. The difference between bases are reproduced reasonably well although both renormalised and power expansions yield too large inaccuracies for small values of  $\varepsilon_J$ . Both numerical and analytical inaccuracies for the a-basis lie approximately half-way between the inaccuracies of the b-basis and 240-state basis but the numerical inaccuracy approaches the larger inaccuracy produced by the 240-state basis for larger values of  $\varepsilon_J (> 0.05)$ .

When considering general results one should compare the diamonds from 240-state basis and crosses from the renormalised unrestricted calculation. Although the renormalised calculation slightly overestimates the inaccuracy for the whole region, the overestimation is well under control for all values of  $\varepsilon_J$ . In addition the scaling of the inaccuracy by  $\varepsilon_J^3$  exaggerates the error for small  $\varepsilon_J$ .

The inset of Fig. 6 shows the numerical and renormalised inaccuracies for  $N = 7$ . Although the results may seem poor at the first glance, one should bear in mind that the 336-states basis is a mix between the a- and b-basis for  $N = 7$  yielding even smaller inaccuracy than the b-basis. This basis was used because the convergence of the inaccuracy was best for this basis and the full diagonalisation required was possible. We have collected the numerical and renormalised inaccuracies for specific values of  $\varepsilon_J$  in Table II. We have also tried to estimate the inaccuracy for the huge  $N = 7$  c-basis based on the power expansions at the degeneracy point. Because the importance of the higher order corrections is more pronounced for  $N = 7$  than for  $N = 5$  the estimates have large error bars for  $\varepsilon_J > 0.15$ . In general we may conclude that the renormalisation seems to be able to reproduce the behaviour of the inaccuracy reasonably well for all  $N$  and  $\varepsilon_J$  in the Coulomb blockade regime.

Basis effects can also be seen in the renormalisation coefficients shown in Fig. 5. We have tabulated their values in Table III for a-, b- and c-bases in cases  $N \geq 6$ . The largest matrix we could diagonalise was the  $2695 \times 2695$ -matrix for the  $N = 7$  c-basis. The basis effects are quite small for  $\varepsilon_J = 0.1$  but for  $\varepsilon_J = 0.2$  they are more visible. In any case the table clearly shows that the maximal supercurrent differs considerably from the simple approximation if the array is longer or if  $\varepsilon_J$  is not very small.

## V. INHOMOGENEITY IN THE ARRAY

In this section we will derive the lowest order contributions for the pumping inaccuracy and the supercurrent on the saw-tooth gating path. The Hamiltonian operator is constructed as follows. First we choose the value of  $\varepsilon_J$  and select  $N$  numbers  $c_k$  satisfying the condition  $\sum_{k=1}^N (1/c_k) = N$ . The capacitance for junction  $k$  is  $C_k = c_k C$ . General considerations imply that the quantity  $E_J E_C$  is approximately constant for all junctions in an array. The Josephson energy is inversely proportional to the normal state resistance  $R_T$  of the junction and  $E_C$  is inversely proportional to the capacitance of the junction. Since  $R_T$  is inversely proportional and capacitance directly proportional to the area of the junction, the product is approximately constant for different junctions in the array. (This argument works only for junctions fabricated in the same batch; otherwise the constants of proportionality are different.)

Thus we will choose  $E_{J,k} = c_k E_J$  in the tunnelling Hamiltonian  $H_J$ . Numerical calculations can now proceed immediately by using the general charging energy (15) with bias voltage  $V$  set to zero for the diagonal matrix elements.

We will try to evaluate and limit the deviations from the homogeneous result in terms of the inhomogeneity. Thus we define the inhomogeneity index of the array,  $X_{\text{inh}}$ , as the root mean square deviation of the quantities  $1/c_k$ . By choosing  $b_k \equiv 1/c_k - 1$  we can write

$$X_{\text{inh}} = \left( \frac{1}{N} \sum_{k=1}^N b_k^2 \right)^{1/2}. \quad (36)$$

The inhomogeneity index is meaningful only if the  $b_k$  are relatively small ( $\leq 0.3$  to  $0.5$ ) but this is easily achieved in experiments by the current technology. The quadratic nature of the index means that one major flaw outweighs several small ones.

Now let us evaluate the charging energies for the states included in the calculation of the inaccuracy and the supercurrent on the saw-tooth gating path. The lowest order corrections are obtained by setting  $a_0 = 0$ ,  $b_0 = c_r$  and evaluating the coefficients  $a_1$  and  $b_{-1}$ . If the current leg is the  $r^{\text{th}}$  leg then junction  $r$  connects the two states that become degenerate while pumping. Let us denote the initial state by  $|0\rangle$ , the final state by  $|r\rangle$  and the relative position between these two states by  $x$ . All the required states can be expressed as  $|\pm(s)\rangle$  for  $s = 0, 1, \dots, N-1$ . For a given state  $|\pm(s)\rangle$  let  $\{l_k\}_{k=1}^s$  be the indices ( $\neq r$ ) of the junctions one has to tunnel through to reach the state. The charging energy can be expressed simply as

$$E_{\text{ch}}^{\pm(s)}(x) = \frac{E_C}{N} \left[ (N/c_r - 1/c_r^2) x^2 + (s + B) ((N - s) \pm 2x(1 + b_r) - B) \right] \quad (37)$$

where  $B \equiv \sum_{k=1}^s b_{l_k}$  and  $x \in [0, 1]$  is the relative position on the current leg. The charging energy for the state  $|r\rangle$  is  $E_C(N/c_r - c_r^{-2})(1 - x)^2/N$ . The charging energies for the homogeneous array are obtained by setting  $b_k \equiv 0$  and the energies at the degeneracy point by setting  $x = \frac{1}{2}$ .

The charging energy differences can easily be read from Eq. (37) since the charging energy of the ground state is included in all cases. Let  $\sigma$  denote a permutation of the set  $\{1, 2, \dots, N\} \setminus \{r\}$  and  $\sigma(k)$  the set of  $k$  first elements in  $\sigma$ .<sup>2</sup> The lowest order approximation of the pumped charge now reads

$$\frac{Q_p}{-2e} = 1 - (K \cos \phi) \sum_{r=1}^N \sum_{\sigma} \frac{c_r^{-2}}{\prod_{s=1}^{N-2} \Delta E_{s,\sigma}}. \quad (38)$$

where  $K \equiv \left( \frac{NE_J}{2E_C} \right)^{N-2} \prod_{k=1}^N c_k$  and

$$\Delta E_{s,\sigma} = (s + B_{\sigma(s)})(N - s - 1 - b_r - B_{\sigma(s)}). \quad (39)$$

In the limit  $X_{\text{inh}} \rightarrow 0$  we find that Eq. (38) yields inaccuracy  $(N\varepsilon_J/2)^{N-2}N(N-1)/(N-2)!$  as required. The inaccuracy is invariant under arbitrary permutations of the set  $\{c_k\}$  which has been crossverified in numerical calculations which now have to span over all  $N$  legs. We also showed that pumped charge may be evaluated for any of the  $N$  junctions but far better numerical convergence is obtained by using the average supercurrent operator  $I_S$ .

The inaccuracy produced by a junction with capacitance  $C_k$  larger than  $C$  is smaller than average and vice versa. By evaluating Eq. (38) for each  $r$  separately and comparing to the numerical result for each leg we see that even these partial results are reproduced well. Even better agreement is achieved by comparing the ratio between the inhomogeneous result Eq. (38) and the homogeneous result  $(N\varepsilon_J/2)^{N-2}N(N-1)/(N-2)!$  to the ratio between the inhomogeneous and the homogeneous numerical result. This comparison should be used since although higher order corrections do not scale exactly as the lowest order correction, their behaviour is nevertheless somewhat similar. In Fig. 7 these ratios are plotted as functions of  $X_{\text{inh}}$  in cases  $N = 4$  and  $N = 5$ . For  $N = 4$  and  $N = 5$  we have used values  $\varepsilon_J = 0.01$  and  $\varepsilon_J = 0.03$  and bases with 16 and 80 states, respectively. The agreement between analytical and numerical results is good.

In order to limit the deviations from the lowest order homogeneous inaccuracy as a function of  $X_{\text{inh}}$  we have used the analytical expression only since numerical simulations would be extremely time-consuming, especially for  $N \geq 6$ . For each length of the array ( $4 \leq N \leq 7$ ) 50 sets of  $c_k$  were chosen from normal distribution with width 0.15 and center at 1. Each set was then normalised and the inhomogeneous inaccuracy was calculated for those sets with  $X_{\text{inh}} < 0.2$  (about 90 % of the sets). The corresponding ratios are shown in Fig. 8. The spread in the ratios for similar inhomogeneity indices grows with increasing  $N$  and also increasing  $X_{\text{inh}}$ . As a conclusion one might say that if  $X_{\text{inh}}$  is less than 0.15 the deviation is less than 40 %. This result should remain valid up to  $\varepsilon_J \approx 0.1$  since the deviation from the lowest order result at 0.1 is of the order of 10 %. Dashed lines show approximate limits for minimum and maximum deviations for array lengths of 4 to 7. The limit  $X_{\text{inh}} < 0.15$  seems to be reasonable for the current technology at capacitances of the order of 1 fF.

The lowest order supercurrent may be estimated as follows. Let  $|\vec{n}_0\rangle$  be the lower one of the two states that become degenerate on the current leg. The other degenerate state is  $|\vec{n}_0 + r\rangle$  which will be the main component of the ground state for  $x \geq 0.5$ . The ground state energy for the “improved” choice in the renormalisation is lowered by  $\Delta E(x) = \frac{1}{2}(E_r^2 + c_r^2 E_J^2)^{1/2} - c_r E_J/2$  where

<sup>2</sup>The notation  $\{1, 2, \dots, N\} \setminus \{r\}$  stands for the set of all positive integers up to  $N$  excluding  $r$ .

$E_r = E_C(N/c_r - c_r^{-2})|1 - 2x|/N$  is the charging energy difference between these states.

Let us assume  $x \leq 0.5$ . Then intermediate states after  $s$  steps are in the class  $|\vec{n}_0 + (s)\rangle$  or  $|\vec{n}_0 + r + (s-1)\rangle = |\vec{n}_0 - (N-s)\rangle$ ,  $s = 1, \dots, N-1$ . Let  $\sigma$  and  $\sigma(s)$  be as in the inaccuracy calculation. The lowest order supercurrent on leg  $r$  then reads

$$\langle I_S \rangle_{(r,x)} = \sum_{\sigma} \sum_{l=1}^N \frac{(I_c \sin \phi) (E_J/2)^{N-1} \prod_{k=1}^N c_k}{\left( \prod_{m=1}^{l-1} \Delta E^{\sigma(m)} \right) \left( \prod_{m=l}^{N-1} \Delta E^{r+\sigma(m-1)} \right)}, \quad (40)$$

where  $r$  is the leg,  $x$  is the relative position on the leg and

$$\begin{aligned} \Delta E^{\sigma(s)} &= E_{\text{ch}}^{(s)}(x) - E_{\text{ch}}^{(0)}(x) + \Delta E(x), \\ \Delta E^{r+\sigma(s)} &= E_{\text{ch}}^{-(N-s-1)}(x) - E_{\text{ch}}^{(0)}(x) + \Delta E(x), \\ \Delta E^{r+\sigma(0)} &= E_{\text{ch}}^{-(N-1)}(x) - E_{\text{ch}}^{(0)}(x) + 2\Delta E(x), \end{aligned}$$

where  $s = 1, \dots, N-1$ . The correction  $2\Delta E(x)$  in the case of the other degenerate state occurs because both charge eigenstates are included in the truncated basis. For  $x \geq 0.5$  Eq. (40) may be used after performing a transformation  $c_k \rightarrow \tilde{c}_k = c_{N+1-k}$  ( $r \rightarrow N+1-r$ ) and  $x \rightarrow \tilde{x} = 1-x$ . If  $X_{\text{inh}}$  is small the current is essentially symmetric around the degeneracy point.

In an a-basis state  $|\vec{n}_0 + (s)\rangle$  is not included if the tunnelling vector  $\vec{\delta}_{r-1}$  ( $N$  for  $r=1$ ) is included in  $(s)$ . Terms including such a state must be discarded thus diminishing the supercurrent which is clearly shown in Fig. 4. In Fig. 9 analytical and numerical supercurrents for  $N=6$  b-basis are shown. Each curve has a different  $X_{\text{inh}}$  and also  $\varepsilon_J$  was chosen randomly between 0.02 and 0.06 as seen from the different widths of the peak. The numerical and analytical results practically coincide.

## VI. INACCURACY AND THE ACCURACY OF GATING

Above we have assumed ideal gating with infinite accuracy. In reality one must adjust the gate voltages which can only be done to a certain precision. For simplicity we assume an uniform  $N$  pump and the initial gate voltage as  $\vec{q} = 0$ . As shown above and in Ref. 4 the amount of charge we carry through the system in the first leg is approximately  $(-2e)(1/N - b_{-1}\varepsilon_J^{N-2} \cos \phi)$ . For larger  $N$  this inaccuracy becomes vanishingly small especially if  $\varepsilon_J \ll 1$ .

In the absence of the supercurrent the transferred charge is exactly given by the changes in the expectation values of the charge. Due to symmetry on the saw-tooth gating path only one pair of charge expectation values may differ from zero and the sum of the normalised ascending and descending gate charge expectation values is exactly unity.

We have evaluated the expectation value of the normalised charge for a homogeneous array by first evaluating the third order renormalised eigenenergy. Then we have expanded the wave functions to include all states that can be reached by at most two steps from the two states that become degenerate at the half-way point. All amplitudes from up to three steps were taken into account. Since a c-basis includes all the states mentioned above we compared the amplitudes to the corresponding amplitudes in wave functions and found that they agree well. The agreement is good regardless of the values of  $\phi$ ,  $\varepsilon_J$  or the value of the normalised ascending gate voltage.

This is graphically depicted in Fig. 10 which shows the resultant deviation of the expectation value of the charge due to an error in one of the normalised gate voltages. The deviation is almost linear in the the normalised ascending gate voltage, and quadratic in  $\varepsilon_J$ . The dependence on the length of array is weaker but noticeable. A tiny error in the charge expectation value is induced by the small inbalance of the basis states included in the summation but it can not be seen in Fig. 10.

Because actually the array need not be homogeneous, nor are we able to fix all other normalised gate voltages to an integer value the cumulative effect may be larger or cancellations may reduce it. In any case the gating inaccuracy may overwhelm the original pumping inaccuracy for relatively small errors in the gating voltages, especially for longer arrays. The difference in the charge transfer due to non-exact gating as compared to the ideal case depends on the deviation of the gate voltages. If the deviation is related to one tunnel junction only, the small but non-zero value of the normalised gate voltage  $x$  induces charge transfer  $\Delta Q_g \approx a(N)x\varepsilon_J^2$  as compared to ideal case. Here  $a \sim 0.05$  is nearly constant. Comparing this charge transfer to the pumping inaccuracy one sees that the inaccuracies are of the same order when

$$x \sim \left( \frac{N}{2} \right)^{N-2} \frac{20N(N-1)}{(N-2)!} \varepsilon_J^{N-4}, \quad (41)$$

which becomes very small for large  $N$  and small  $\varepsilon_J$ . On the other hand the accuracy required by metrological applications<sup>2</sup> is of the order of  $10^{-8}$ , which only requires  $x \sim 2 \cdot 10^{-7} \varepsilon_J^{-2}$ . This should be more reasonable a demand.

## VII. CONCLUSIONS

We have considered pumping of Cooper pairs in an array of Josephson junctions in an environment with vanishing impedance. We have successfully evaluated higher order corrections to the supercurrent and pumped charge in the absence of external bias voltage. The renormalisation method used in this article has proven to be quite accurate and effective. Because even the size of the minimal a-basis rapidly grows beyond the capacity of computers, accurate analytical expressions have to be used in order to circumvent this problem.

In addition to the higher order corrections for a homogeneous array we are able to reliably evaluate the effect of inhomogeneity in the array, at least in the leading order. Thus we can limit the variation in the inaccuracy as a function of the inhomogeneity in the array although this would not have been possible numerically.

The inaccuracy of gating can be shown to be another error source when pumping Cooper pairs. We have not taken into account the effects due to environment and it remains to be seen how severely the present results will be modified. The influence of the environment and the measurement of the transported charge will be the next steps in the more complete description of the Cooper pair pumps.

TABLE I. Coefficient  $b_{-1}^{(N)}$  for a-, b- and c-basis and  $b_1^{(N)}$  for c-basis in cases  $N = 3$  to  $N = 8$ . The expressions have been calculated by using the charging energy of the degenerate states in the denominator. Exact values are given as fractions when value fits into the column. Only the full c-basis value has been evaluated.

N	$b_{-1,a}^{(N)}$	$b_{-1,b}^{(N)}$	$b_{-1,c}^{(N)}$	$b_{1,c}^{(N)}$
3	9/4	57/8	69/8	3/4
4	63/2	436/10	513/10	5/2
5	83.189	106.44	125.54	5.792
6	176.78	217.07	261.52	459/40
7	339.51	405.5	497.62	20.834
8	—	—	894.45	35.781

<sup>1</sup> H. Pothier, P. Lafarge, C. Urbina, D. Esteve and M.H. Devoret, *Europhys. Lett* **17**, 249 (1992).

<sup>2</sup> M.W. Keller, J.M. Martinis, N.N. Zimmerman and A.H. Steinbach, *Appl. Phys. Lett.* **69**, 1804 (1996); M.W. Keller, J.M. Martinis and R.L. Kautz, *Phys. Rev. Lett.* **80**, 4530 (1998).

<sup>3</sup> M.W. Keller, Ali L. Eichenberg, John M. Martinis and Neil M. Zimmerman, *Science* **285**, 1716 (1999).

<sup>4</sup> J.P. Pekola, J.J. Toppari, M. Aunola, M.T. Savolainen and D.V. Averin, *Phys. Rev. B* **60**, R9931 (1999).

<sup>5</sup> L.J. Geerligs, S.M. Verbrugh, P. Hadley, J.E. Mooij, H. Pothier, P. Lafarge, C. Urbina, D. Esteve and M.H. Devoret, *Z. Phys. B: Condens. Matter* **85**, 349 (1991).

<sup>6</sup> P.J. Ellis and E. Osnes, *Rev. Mod. Phys.* **49**, 777 (1978).

<sup>7</sup> M. Hjorth-Jensen, in *Advances in Quantum Many-Body Theory*, Vol. 2, eds. R. Bishop and N.R. Walet, (World Scientific, Singapore), in press.

<sup>8</sup> M. Hjorth-Jensen, T.T.S. Kuo and E. Osnes, *Physics Reports* **261** 125 (1995).

<sup>9</sup> T.T.S. Kuo and E. Osnes, *Folded-Diagram Theory of the Effective Interaction in Atomic Nuclei*, Springer Lecture Notes in Physics, (Springer, Berlin, 1990) Vol. **364**; T.T.S. Kuo, *Lecture Notes in Physics; Topics in Nuclear Physics*, eds. T.T.S. Kuo and S.S.M. Wong, (Springer, Berlin, 1981) Vol. **144**, p. 248.

<sup>10</sup> I. Lindgren and J. Morrison, *Atomic Many-Body Theory*, *J. Phys. B: At. Mol. Opt. Phys.* **24** (1991) 1143.

TABLE II. Comparison between scaled numerical and renormalised inaccuracies for specific values of  $\varepsilon_J$ . For the numerical inaccuracy has been evaluated for a 240-state and a 336-state basis and for  $N = 5$  and  $N = 7$ , respectively. We have also tried to evaluate the expected inaccuracy for the 2695-state c-basis for  $N = 7$ .

$\varepsilon_J$	$N = 5$		$N = 7$		
	num.	ren.	num	appr.	ren.
0.05	50.53	51.36	176.38	$178 \pm 1$	180.84
0.1	46.55	48.70	158.22	$162 \pm 2$	169.90
0.15	40.76	43.63	134.34	$138 \pm 3$	149.10
0.2	33.98	36.82	109.04	$115 \pm 4$	121.54

TABLE III. Renormalisation coefficients for the maximal supercurrent for different bases and for larger values of  $N$ . The differences are relatively small even for the larger ratio  $\varepsilon_J = 0.2$ . Non-renormalised theoretical supercurrent is  $I_C \sin(\phi/N)/N$ . The largest basis used was the c-basis for  $N = 7$  since available memory was insufficient for larger ones.

$N$	$\varepsilon_J$	a-basis	b-basis	c-basis
6	0.1	1.485	1.488	1.491
6	0.2	1.881	1.897	1.913
7	0.1	1.589	1.591	1.596
7	0.2	2.072	2.087	2.113
8	0.1	1.689	1.691	—
8	0.2	2.256	2.271	—
9	0.1	1.786	1.788	—
9	0.2	2.435	2.448	—
10	0.1	1.881	—	—
10	0.1	2.601	—	—

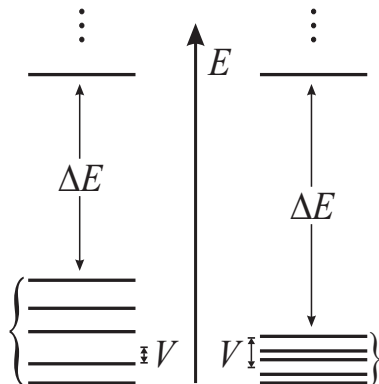


FIG. 1. Schematic view of two few-state dominant systems. On the right-hand-side all low-lying levels are closely packed in energy while on the left-hand-side the spread is large as compared to  $V \equiv V_{\max}$ . In both cases the requirements for few-state dominance are well satisfied.

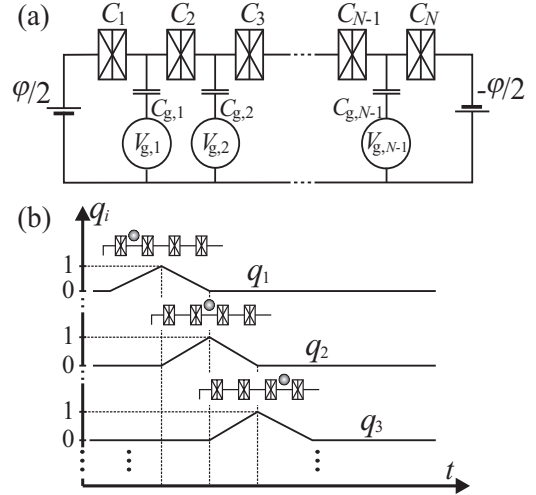


FIG. 2. (a) A schematic drawing of a gated Josephson array of  $N$  junctions. In pumping Cooper pairs, gate voltages  $V_{g,k}$  are operated cyclically.  $C_k$  are the capacitances of the junctions and  $C_{g,k}$  are the gate capacitances. b) A train of gate voltages to carry a charge in a pump. Here  $q_k = -C_{g,k}V_{g,k}/2e$ . The dominant state at the turning points of gate voltages are also shown.

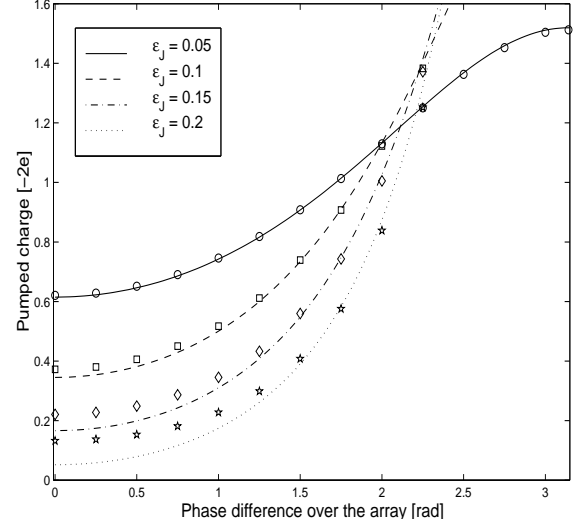


FIG. 3. The pumped charge  $Q_p/(-2e)$  as a function of the total phase difference over the array  $\phi$  for some values of  $\varepsilon_J$ . Curves denote analytical values and separate symbols numerical values. Pumped charge is symmetric in  $\phi$  and its period is  $2\pi$ .

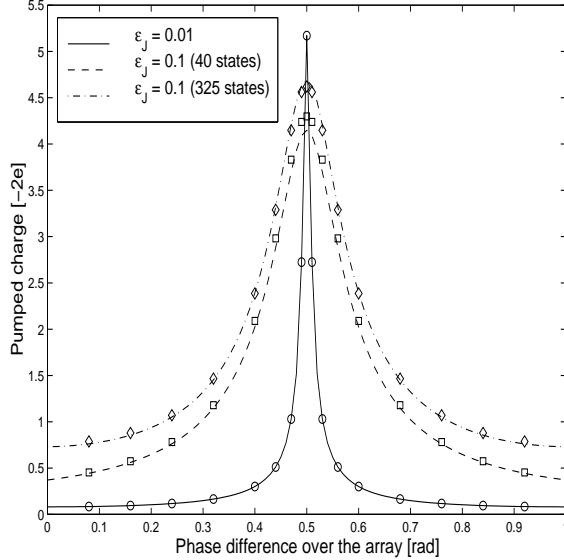


FIG. 4. The maximal value for the supercurrent in units  $I_C \varepsilon_J^3$  for  $N = 5$ . For clarity a basis with 40 states was used although it is not large enough to support full supercurrent in the lowest order. Only coefficients  $b_{-1}$  and  $a_1$  have been taken into account which can be seen from the underestimation of the supercurrent at the degeneracy point. For the large basis with 325 states the supercurrent is reproduced very nicely. Curves denote analytical values and markers numerical values. In case  $\varepsilon_J = 0.01$  the differences between bases can hardly be seen even at the degeneracy point.

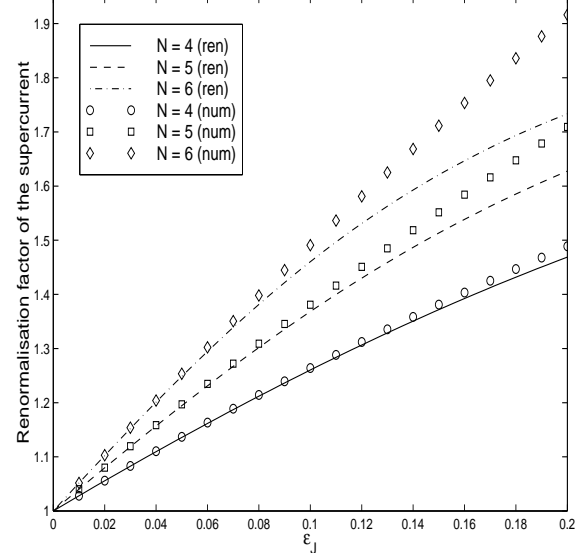


FIG. 5. The renormalisation coefficient of the supercurrent as a function of  $\varepsilon_J$  at the resonance point for phase difference  $\phi = \pi$  yielding the maximal supercurrent  $I_c \sin(\pi/N)/N$  for the array. Curves agree with the numerical results for small values of  $\varepsilon_J$ . The deviations at higher values are due to higher order corrections. The number of the states used in the numerical calculation are 100, 325 and 966 for  $N = 4$ ,  $N = 5$  and  $N = 6$ , respectively.

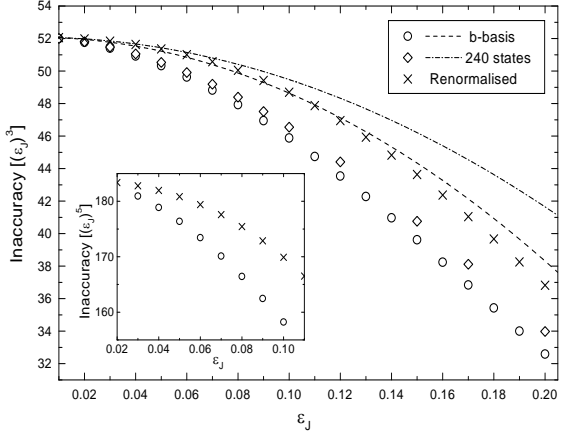


FIG. 6. The pumped charge  $Q_p/(-2e)$  as a function of  $\epsilon_J$  for different bases and  $N = 5$ . Curves denote power expansions and separate symbols numerical or renormalised values. The inaccuracy is given in units  $\epsilon_J^3$  and the phase difference used is  $\phi = 0$ . The inaccuracy for the a-basis lies approximately half-way between the b-basis and the 240-state basis both for numerical and analytical calculations. The scaling allows us to compare the inaccuracies more clearly but it simultaneously exaggerates the absolute errors. Inset shows the results for the  $N = 7$ , 336-state basis. This basis was optimal in terms of the convergence of the inaccuracy. Although the difference between the numerical and renormalised results may look surprisingly large it should be pointed out that the actual error is much smaller. The basis used is a hybrid between an a-basis and a b-basis yielding even smaller an inaccuracy than the b-basis shown in the main figure.

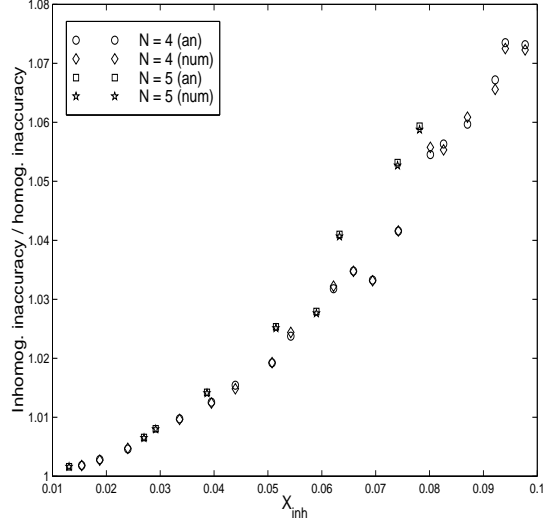


FIG. 7. The ratios between the inhomogeneous and the homogeneous inaccuracies from analytical and numerical calculations as functions of the inhomogeneity index  $X_{\text{inh}}$ . The ratio  $\epsilon_J$  used for  $N = 4$  and  $N = 5$  is 0.01 and 0.03, respectively.

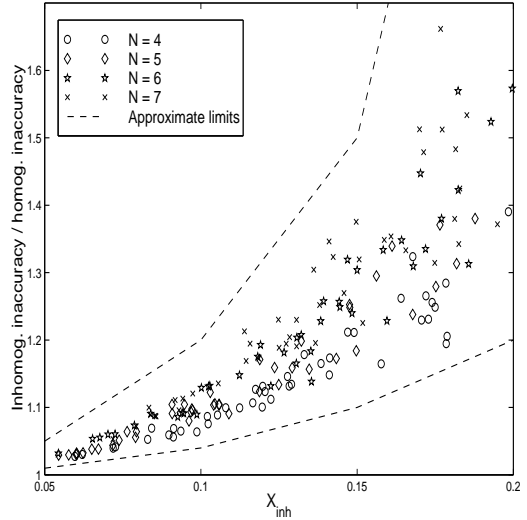


FIG. 8. The ratios between inhomogeneous and homogeneous inaccuracies from analytical calculations as functions of  $X_{\text{inh}}$  for  $N = 4$  to  $N = 7$ . Approximate limits outside which no data points are expected to occur have been drawn, also.

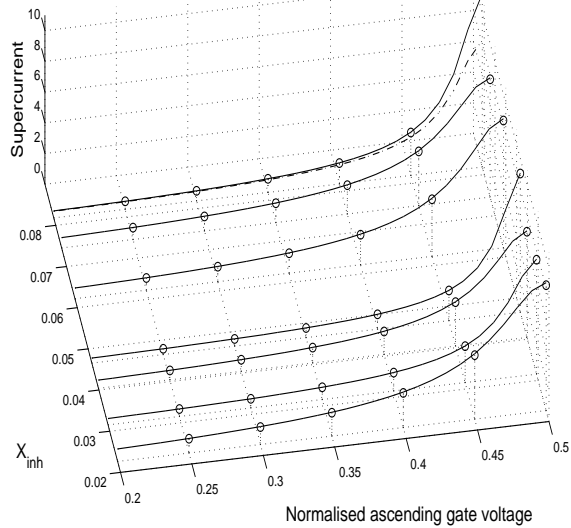


FIG. 9. A three-dimensional plot of the supercurrent for  $N = 6$  and phase difference  $\phi = \pi/2$  in units  $I_c \epsilon_J^4$  as a function of  $X_{inh}$ . The gate voltage are chosen from the first leg of the saw-tooth gating path. Junction capacitances have been chosen randomly as well as the ratios  $\epsilon_J$  which lie between 0.02 and 0.06. Solid curves denote analytical values and discrete symbols numerical values. The modifications of the supercurrent are well reproduced for larger inhomogeneities as shown by the variation of the supercurrent at the degeneracy point and the difference between the solid curve and the dash-dot curve of the homogeneous case for the largest  $X_{inh}$ . Dotted curves connect the numerical points to the  $(x, X_{inh})$ -plane.

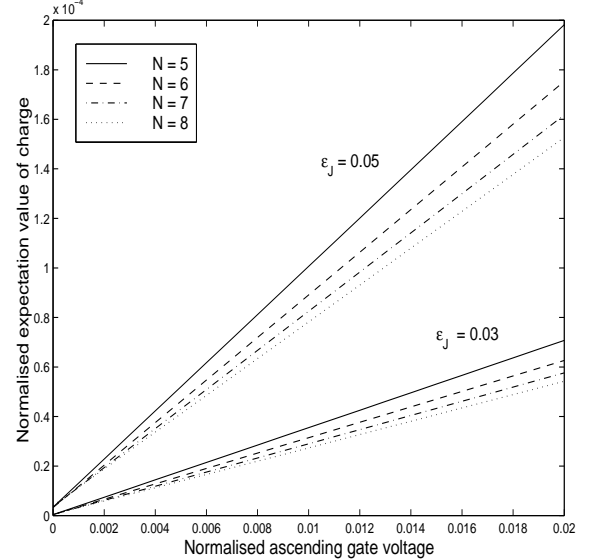


FIG. 10. The expectation value of the ascending charge as a function of the normalised ascending gate voltage for different lengths of the array  $N$  and two different values of  $\epsilon_J$ . The charge is linearly dependent on the ascending gate voltage and quadratically dependent on  $\epsilon_J$ . The  $N$ -dependence is much weaker but noticeable.